INTENTIONAL JAMMING SUPPRESSION IN A FREQUENCY-DOMAIN ULTRA-WIDEBAND MULTICARRIER COMMUNICATION RECEIVER

Sebastian Hoyos†, Brian M. Sadler‡, Gonzalo R. Arce†

†University of Delaware, Department of Electrical and Computer Engineering, 140 Evans Hall, Newark, DE 19716, hoyos@ee.udel.edu, arce@ee.udel.edu

‡Army Research Laboratory, AMSRD-ARL-CI-CN 2800 Powder Mill Rd. Adelphi, MD 20783 bsadler@arl.army.mil

ABSTRACT

This paper presents suppression of intentional jamming in an ultra-wideband multicarrier communication receiver based on analog to digital conversion (ADC) in the frequency domain. The samples of the spectrum of the received signal are used in the digital receiver to estimate the transmitted symbols through a matched filter operation in the discrete frequency domain. The proposed receiver is aimed at the reception of high information rates in a multicarrier signal with very large bandwidth. Thus, the receiver architecture provides a solution to some of the challenging problems found in the implementation of conventional wideband multicarrier receivers based on time-domain ADC, and it is directly applicable to multicarrier ultra-wideband communication receivers. Additional advantages of the proposed receiver include the possibility of optimally allocating the available number of bits for the A/D conversion across the frequency domain samples, narrowband interference suppression based on the MMSE solution that can be directly carried out in the frequency domain, and inherent robustness to frequency offset which makes it an attractive solution when compared with traditional multicarrier receivers.

1. INTRODUCTION

In multicarrier communications systems, the available channel bandwidth is efficiently used by subdividing it into a number of subchannels with sufficiently small bandwidth such that each subchannel frequency response is non-frequency selective [1–3]. Such systems have been successfully implemented, with orthogonal frequency division multiplexing (OFDM) the most well-known approach [4–6]. The OFDM receiver architecture is essentially based on conventional time-domain analog to digital conversion followed by a discrete Fourier transform (DFT) that provides the estimates of the transmitted symbols. However, if the bandwidth of the multicarrier signal is increased in order to achieve higher data rates and accommodate larger numbers of users, as it has been proposed in UWB communications systems, the implementation of the front-end conventional time-domain ADC operating at Nyquist rate presents a significant challenge. Additionally, the use of conventional UWB multicarrier communication systems in military applications has the potential risk of being affected by intentional jamming introduced through narrowband and wide-band interference signals.

Prepared through collaborative participation in the Communications and Networks Consortium sponsored by the U. S. Army Research Laboratory under the Collaborative Technology Alliance Program, Cooperative Agreement DAAD19-01-2-0011.

The multicarrier receiver presented in this paper provides a solution that parallelizes the analog to digital conversion, efficiently reducing the operational speed of the ADC even if signals with very large bandwidths are used for the transmission of high data rates. The new receiver architecture is based on an analog to digital converter in the frequency domain [7] that takes N samples of the spectrum of the received signal every T_c seconds. The samples of the signal spectrum are used in a digital receiver based on a bank of discrete-frequency matched filters that calculate the estimates of the transmitted symbols. The system proposed here is capable of suppressing jamming signals by the direct application of either frequency bin excision or a minimum mean-square solution with the data samples provided by the frequency domain ADC. These anti-jamming techniques are useful for combat communication systems and are under investigation by the authors in the communications and networks consortium sponsored by the U.S. Army Research Laboratory under the Collaborative Technology Alliance Program, Cooperative Agreement DAAD19-01-2-0011.

2. ANALOG TO DIGITAL CONVERSION IN THE FREQUENCY DOMAIN

Figure 1(a) shows the block diagram of the ADC in the frequency domain [8] in which signal projection over the complex exponential functions allows sampling of the continuous-time signal spectrum at the frequencies $F_n \mid_{n=0}^{N-1}$, leading to the set of frequency coefficients

$$c_n = \int_0^{T_c} s(t) e^{-j2\pi F_n t}\, \mathrm{d}t, \qquad n = 0, \cdots, N-1. \quad (1)$$

The coefficients $c_n \mid_{n=0}^{N-1}$ are then quantized by a set of quantizers $Q_n \mid_{n=0}^{N-1}$, which in turn produce the ADC output digital coefficients $\hat{c}_n = Q_n(c_n) \mid_{n=0}^{N-1}$. The conversion frequency sample spacing $\Delta F_c = F_n - F_{n-1}$ complies with $\Delta F_c \leq \frac{1}{T_c}$ in order to avoid aliasing in the discrete-time domain. Thus, the optimal number of coefficients N necessary to fully sample the signal spectrum with bandwidth W is given by

$$N = \left\lceil \frac{W}{\Delta F_c} \right\rceil \geq \lceil W T_c \rceil, \quad (2)$$

where the operator $\lceil\ \rceil$ is used to ensure that N is the closest upper integer that avoids discrete-time aliasing.

Report Documentation Page

Form Approved
OMB No. 0704-0188

1. REPORT DATE	2. REPORT TYPE	3. DATES COVERED
00 DEC 2004	**N/A**	**-**

4. TITLE AND SUBTITLE	
Intentional Jamming Suppression In A Frequency-Domain Ultra-Wideband Multicarrier Communication Receiver	5a. CONTRACT NUMBER
	5b. GRANT NUMBER
	5c. PROGRAM ELEMENT NUMBER
6. AUTHOR(S)	5d. PROJECT NUMBER
	5e. TASK NUMBER
	5f. WORK UNIT NUMBER
7. PERFORMING ORGANIZATION NAME(S) AND ADDRESS(ES) **University of Delaware, Department of Electrical and Computer Engineering, 140 Evans Hall, Newark, DE 19716; Army Research Laboratory, AMSRD-ARL-CI-CN 2800 Powder Mill Rd. Adelphi, MD 20783**	8. PERFORMING ORGANIZATION REPORT NUMBER
9. SPONSORING/MONITORING AGENCY NAME(S) AND ADDRESS(ES)	10. SPONSOR/MONITOR'S ACRONYM(S)
	11. SPONSOR/MONITOR'S REPORT NUMBER(S)

12. DISTRIBUTION/AVAILABILITY STATEMENT
Approved for public release, distribution unlimited

13. SUPPLEMENTARY NOTES
See also ADM001736, Proceedings for the Army Science Conference (24th) Held on 29 November - 2 December 2004 in Orlando, Florida., The original document contains color images.

14. ABSTRACT

15. SUBJECT TERMS

16. SECURITY CLASSIFICATION OF:			17. LIMITATION OF ABSTRACT	18. NUMBER OF PAGES	19a. NAME OF RESPONSIBLE PERSON
a. REPORT	b. ABSTRACT	c. THIS PAGE			
unclassified	**unclassified**	**unclassified**	**UU**	**5**	

Standard Form 298 (Rev. 8-98)
Prescribed by ANSI Std Z39-18

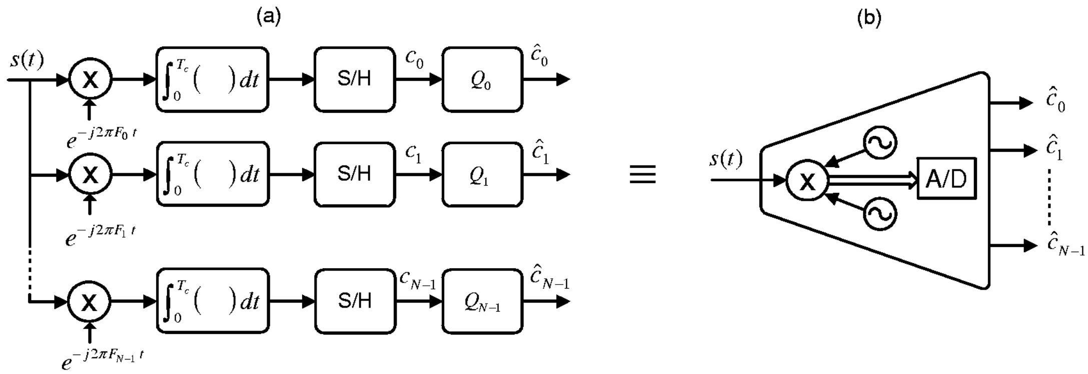

Fig. 1. (a) Block diagram of the analog to digital converter in the frequency domain. (b) Block representation of the ADC in the frequency domain.

A. A/D Conversion of Multicarrier Signals in the Frequency Domain

Let us consider the complex envelope of a multicarrier signal $x(t)$ composed of the sum of S complex exponentials with associated complex amplitude $a_s\,|_{s=0}^{S-1}$

$$x(t) = \sum_{s=0}^{S-1} a_s e^{j2\pi f_s t}, \qquad 0 \le t \le T, \tag{3}$$

where the intercarrier frequency spacing is given by $\Delta F = f_s - f_{s-1} = \frac{1}{T}\ \forall s$. We first notice that by making $T_c = T$, a total of $N = S$ frequency samples of $x(t)$ are needed to recover the coefficients $a_s\,|_{s=0}^{S-1}$. In such a case, the frequency domain ADC is just a simple correlator bank. The problem with choosing $T_c = T$ is that when a large number of carriers are used, twice this number of multiply and integrate devices are needed in the implementation of the correlator bank, which could make the system impractical. Therefore, it is of great interest to investigate cases in which the conversion-time satisfies $T_c < T$. In particular, we chose $T_c = T/M$, with M an integer. We define the signal $x_m(t) = x(t)w_m(t)$,

$$w_m(t) = \begin{cases} 1 & mT_c \le t \le (m+1)T_c \\ 0 & \text{elsewhere} \end{cases} \tag{4}$$

where $m = 0, \cdots, M-1$, and the window $w_m(t)$ has been selected as rectangular for simplicity of the analysis. It is easy to verify that the Fourier transform ($\mathcal{F}$) of $w_m(t)$ is given by $\mathcal{F}\{w_m(t)\} = W_m(F) = \frac{\sin(\pi F T_c)}{\pi F} e^{-j\pi(2m+1)T_c F}$. The Fourier transform of $x_m(t)$, denoted as $X_m(F)$, can be expressed as

$$\begin{aligned} X_m(F) &= \mathcal{F}\{x(t)\} * \mathcal{F}\{w_m(t)\} = \mathcal{F}\left\{\sum_{s=0}^{S-1} a_s e^{j2\pi f_s t}\right\} * W_m(F) \\ &= \left(\sum_{s=0}^{S-1} a_s \delta(F - f_s)\right) * \left(\frac{\sin(\pi F T_c)}{\pi F} e^{-j\pi(2m+1)T_c F}\right) \\ &= \sum_{s=0}^{S-1} a_s \frac{\sin(\pi T_c (F - f_s))}{\pi (F - f_s)} e^{-j\pi T_c (2m+1)(F - f_s)}, \end{aligned} \tag{5}$$

where windowing in time-domain of the signal leads to convolution in frequency domain, which in turn produces bandwidth expansion. Fig. 2(a) shows the signal-bandwidth symbol-period product (WT) versus the ratio between the symbol-period and the conversion-time (T/T_c). This plot shows that the normalized signal bandwidth increases slowly as the extent of segmentation T/T_c is increased. Fig. 2(b) shows the number of coefficients N versus the ratio $M = T/T_c$. The figure shows that even though further segmentation of the multicarrier signal increases the bandwidth of the signal to be A/D converted, even larger reductions in the number of coefficients N is obtained. The favorable trade-off between N and T_c illustrated in Fig. 2(b) is very important in the implementation of the ADC in the frequency domain for multicarrier signals, since it indicates that a practical number of frequency samples N can be obtained by adequately selecting a symbol-period to conversion-time ratio $M = T/T_c$. Additionally, it is interesting to notice that as $M = T/T_c$ is increased, the number of frequency samples N will eventually reach the value 1, which is just the point where the ADC in the frequency domain turns into a DC-level collector. At this point of operation, the ADC samples the DC frequency, which is just the average of the signal over the integration time T_c. Furthermore, as T_c decreases, the signal in the interval T_c approaches a flat level with average equal to any time-domain sample in that interval. So, Fig. 2(b) illustrates the three regions of operation of the ADC of Fig. 1, which are (1) $T_c = T$ which leads to $N = S$, a straightforward correlator bank, (2) $T_c < T$ such that $N < S$, which is the proposed ADC in the frequency domain and (3) $T_c << T$ such that $N = 1$, the conventional time-domain ADC.

3. Multicarrier Communication System Based on Frequency Domain A/D Conversion

Assume that the available channel bandwidth BW is divided into S subchannels of bandwidth BW/S with center frequencies $f_s\,|_{s=0}^{S-1}$. Thus, a block of S symbols $a_s\,|_{s=0}^{S-1}$ is simultaneously transmitted through the channel over a signal

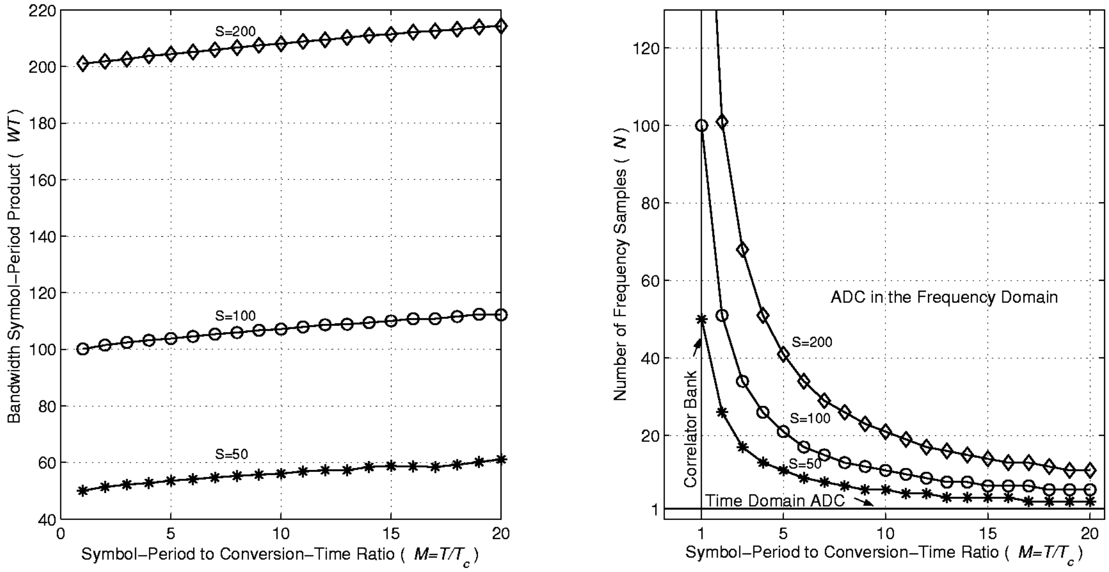

Fig. 2. Characteristics of A/D conversion of multicarrier signals in the frequency domain. (a) Bandwidth symbol-period product vs. Symbol-period to conversion-time ratio ($M = T/T_c$). (b) Symbol-period to conversion-time ratio ($M = T/T_c$)

block time T. The transmitted signal for a block of symbols can be expressed as in Eqn. (3). In OFDM systems, the generation of the transmit signal $x(t)$ is achieved by performing an inverse DFT operation over the block of symbols $a_s\,|_{s=0}^{S-1}$, which are then passed through a D/A converter to generate a continuous-time signal that is then frequency shifted to some desired frequency band.

The signal $x(t)$ is transmitted over a linear communication channel with impulse response $h(t)$ and frequency response $H(f)$. Assuming that the channel is flat in each of the transmission subbands, the received signal can be expressed as follows

$$r(t) = x(t) * h(t) + z(t) \approx \sum_{s=0}^{S-1} a_s e^{j2\pi f_s t} H(f_s) + z(t),\ 0 \le t \le T. \tag{6}$$

where "$*$" indicates continuous-time convolution and $z(t)$ is additive white Gaussian noise (AWGN). In conventional OFDM systems, the received continuous-time signal is first passed through a time-domain A/D converter running at Nyquist rate, and the discrete-time samples are then demodulated by performing a DFT operation. The following subsection presents a fundamentally different approach for the implementation of the multicarrier receiver, based on A/D conversion in the frequency domain.

A. Multicarrier Receiver Based on Analog to Digital Conversion in the Frequency Domain

Figure 3 illustrates the proposed receiver architecture. The ADC in the frequency domain provides the set of samples $R_m(F_n)\,|_{n=0}^{N-1}$ every T_c seconds, where $m = 0, \cdots, M-1$ and the information symbol block period T is related with the A/D conversion-time T_c as $T = MT_c$. We begin by expressing the calculation as a matched filter problem in time domain $\bar{a}_s = \int_0^T r(\tau) g_s^*(\tau)\,\mathrm{d}\tau$, where $\bar{a}_s$ is the estimated symbol associated to the carrier at frequency f_s, $g(t)$ is the impulse response of the matched filter and the output of this filter is sampled at $t = T$. Ideally, the matched filter impulse response is given by

$$g_s^*(t) = e^{-j2\pi f_s t} * h^*(t) \approx e^{-j2\pi f_s t} H^*(f_s),\ 0 \le t \le T \tag{7}$$

where $(\cdot)^*$ indicates complex conjugate, and once again the approximation follows from assuming that the channel frequency response is flat across the subchannels. In order to reflect the effect of segmenting the signal duration time T into M time-slots of duration T_c, we define the following signals

$$r_m(t) = r(t) w_m(t), \quad g_{s,m}(t) = g_s(t) w_m(t), \tag{8}$$

where $m = 0, \cdots, M-1$, and the window $w_m(t)$ is introduced in (4). Using these definitions, the matched filter output can be expressed as

$$\begin{aligned} \bar{a}_s &= \sum_{m=0}^{M-1} \int_{mT_c}^{(m+1)T_c} r(\tau) g_s^*(\tau)\,\mathrm{d}\tau \qquad (9)\\ &= \sum_{m=0}^{M-1} \int_{mT_c}^{(m+1)T_c} r_m(\tau) g_{s,m}^*(\tau)\,\mathrm{d}\tau = \sum_{m=0}^{M-1} \int_{-\infty}^{\infty} r_m(\tau) g_{s,m}^*(\tau)\,\mathrm{d}\tau, \end{aligned}$$

In order to express the matched filter operations in the frequency-domain, the Parseval's theorem is used in (9), leading to

$$\begin{aligned} \bar{a}_s &= \sum_{m=0}^{M-1} \int_{-\infty}^{\infty} r_m(\tau) g_{s,m}^*(\tau)\,\mathrm{d}\tau \\ &= \sum_{m=0}^{M-1} \int_{-\infty}^{\infty} R_m(F) G_{s,m}^*(F)\,\mathrm{d}F, \qquad (10) \end{aligned}$$

where $R_m(F) = \mathcal{F}\{r_m(t)\}$ and $G_{s,m}(F) = \mathcal{F}\{g_{s,m}(t)\}$. Since only N samples of the received signal spectrum are provided by the ADC in the frequency domain, (10) is approximated as

$$\begin{aligned} \bar{a}_s &= \sum_{m=0}^{M-1} \int_{-\infty}^{\infty} R_m(F) G_{s,m}^*(F)\,\mathrm{d}F \qquad (11)\\ &\approx \sum_{m=0}^{M-1} \Delta F_c \sum_{n=0}^{N-1} \left(R_m(F_n) G_{s,m}^*(F_n) + R_m(-F_n) G_{s,m}^*(-F_n) \right), \end{aligned}$$

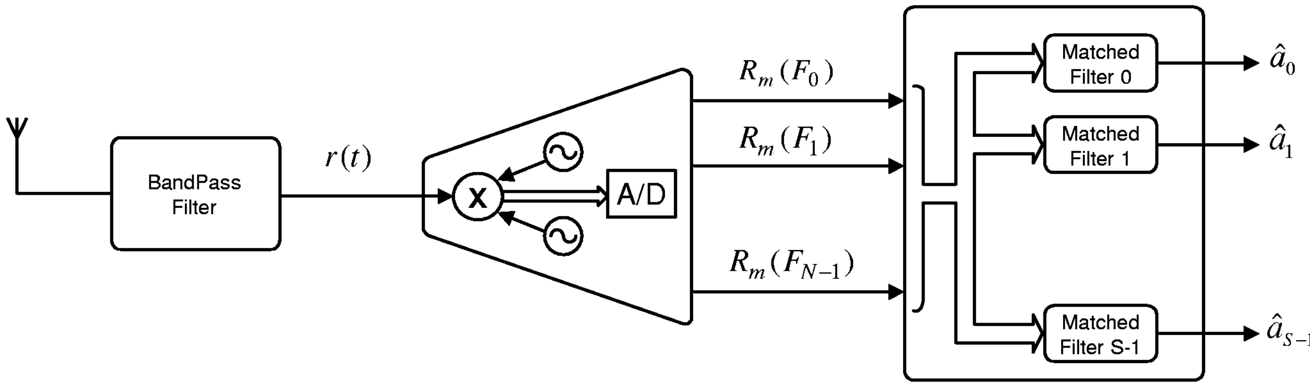

Fig. 3. Block diagram of multicarrier receiver based on ADC in the frequency domain.

where $R_m(\pm F_n)\mid_{n=0}^{N-1}$ and $G_{s,m}(\pm F_n)\mid_{n=0}^{N-1}$ are the samples from the spectrum of $r_m(t)$ and $g_{s,m}(t)$, respectively. Since the received signal is real-valued, we have that $R_m(F_n) = R_m^*(-F_n)$. If the number of frequency samples K, where $K = 2(N-1)$, comply with both no discrete-time aliasing and Nyquist rate, the error introduced in (11) is negligible.

The samples of the spectrum of the segmented matched filter, $G_{s,m}^*(F_n)\mid_{n=0}^{N-1}$, need to be estimated in order to calculate the information symbol estimates in (11). The accuracy of the estimates $\hat{a}_s$ will depend on how close the channel estimates $\hat{G}_{s,m}(F_n)\mid_{n=0}^{N-1}$ are to their true values $G_{s,m}(F_n)\mid_{n=0}^{N-1}$. When the channel estimates are perfect, the signal is free of intercarrier or intersymbol interference, and the number of spectrum samples N satisfies Eqn. (2) which avoids discrete-time aliasing and makes the error in (10) negligible, then the probability of error associated with this receiver will be the same probability of error of a conventionally implemented multicarrier or multichannel communication system.

4. Intentional Jamming Suppression

Narrow band interference (NBI) can affect the received signal degrading the performance of the proposed MC receiver. Denoting $u(t)$ as the NBI signal, and $v_m(t) = u(t)w_m(t)$, the received signal in the interval $mT_c \le t \le (m+1)T_c$ can be expressed as

$$r_m(t) = [x(t) * h(t) + z(t) + u(t)]w_m(t) \approx \left[\sum_{s=0}^{S-1} a_s H(f_s) e^{j2\pi f_s t}\right] w_m(t) + z_m(t) + u_m(t), \quad (12)$$

where $z_m(t) = z(t)w_m(t)$ and $u_m(t) = u(t)w_m(t)$.

The samples provided by the ADC in the frequency domain become

$$R_m(F_n) = \sum_{s=0}^{S-1} a_s H(f_s) \frac{\sin(\pi T_c(F_n - f_s))}{\pi(F_n - f_s)} e^{-j\pi T_c(2m+1)(F_n - f_s)} + Z_m(F_n) + U_m(F_n) = \sum_{s=0}^{S-1} a_s H(f_s) \frac{\sin(\pi T_c(F_n - f_s))}{\pi(F_n - f_s)} \cdot e^{-j\pi T_c(2m+1)(F_n - f_s)} + V_m(F_n). \quad (13)$$

Modelling the NBI term $U_m(F_n)$ as a zero-mean bandlimited Gaussian process, the new variable $V_m(F_n) = Z_m(F_n) + U_m(F_n)$ is a Gaussian random variable with variance given by $No/2 + Jo/2$ if the jammer affects the frequency sample $R_m(F_n)$ or $No/2$ if the jammer does not affect the frequency sample $R_m(F_n)$, where $Jo/2$ is the variance of the NBI. The fractional number of frequency samples affected by the NBI will be denoted as ε, where $0 \le \varepsilon \le 1$. Therefore, the additive noise is no longer white, making the matched filter expression in (9) a suboptimal solution. Better performance can be obtained by using a minimum mean-square error (MMSE) receiver. To simplify the analysis we can assume that a multi-carrier spread spectrum system is used, in which a single information symbol a has been spread out across the subchannels using a code $B^T = [b_0 \cdots b_{S-1}]$, leading to the transmitted symbols $a_s = ab_s\mid_{s=0}^{S-1}$. Let us define the signal $G_m(F_n) = \sum_{s=0}^{S-1} b_s G_{s,m}(F_n)$, which allows to define the $NM \times 1$ vector G with components given by $G_{mM+n} = G_m(F_n)\mid_{m=0}^{M-1}\mid_{n=0}^{N-1}$. The received signal can be expressed in the following convenient vector notation $R = aG + V$, where R is $NM \times 1$ vector with entries $R_{mM+n} = R_m(F_n)\mid_{m=0}^{M-1}\mid_{n=0}^{N-1}$, and similarly V is a $NM \times 1$ vector with entries $V_{mM+n} = V_m(F_n)\mid_{m=0}^{M-1}\mid_{n=0}^{N-1}$. The MMSE receiver is given by

$$C^T = \sigma_a^2 G^H \left(\mathcal{R}_{VV} + \sigma_a^2 G G^H\right)^{-1} = \frac{\sigma_a^2}{1 + \sigma_a^2 + G^H \mathcal{R}_{VV}^{-1} G} G^H \mathcal{R}_{VV}^{-1} \quad (14)$$

where $\sigma_a^2 = E\{|a|^2\}$ and $\mathcal{R}_{VV} = E\{VV^H\}$ is the noise autocorrelation matrix. The signal to noise ratio of the MMSE receiver output is given by

$$\mathrm{SNR}_{\mathrm{MMSE}} = \frac{E\{|aC^T G|^2\}}{E\{|C^T V|^2\}} = \sigma_a^2 G^H \mathcal{R}_{VV}^{-1} G. \quad (15)$$

Figure 4 shows the SNR and the bit error rate (BER) for both the matched filter and MMSE receivers for different values of the fractional number of frequency samples hit by NBI (ε), different values of $\mathrm{SNR}_{\mathrm{AWGN}} = 10\log_{10}(E_b/N_o)$ where $E_b = \sigma_a^2 \|G\|^2$, and a fixed AWGN to NBI variance ratio $10\log_{10}(N_o/J_o) = -10$ dB. As expected, the MMSE

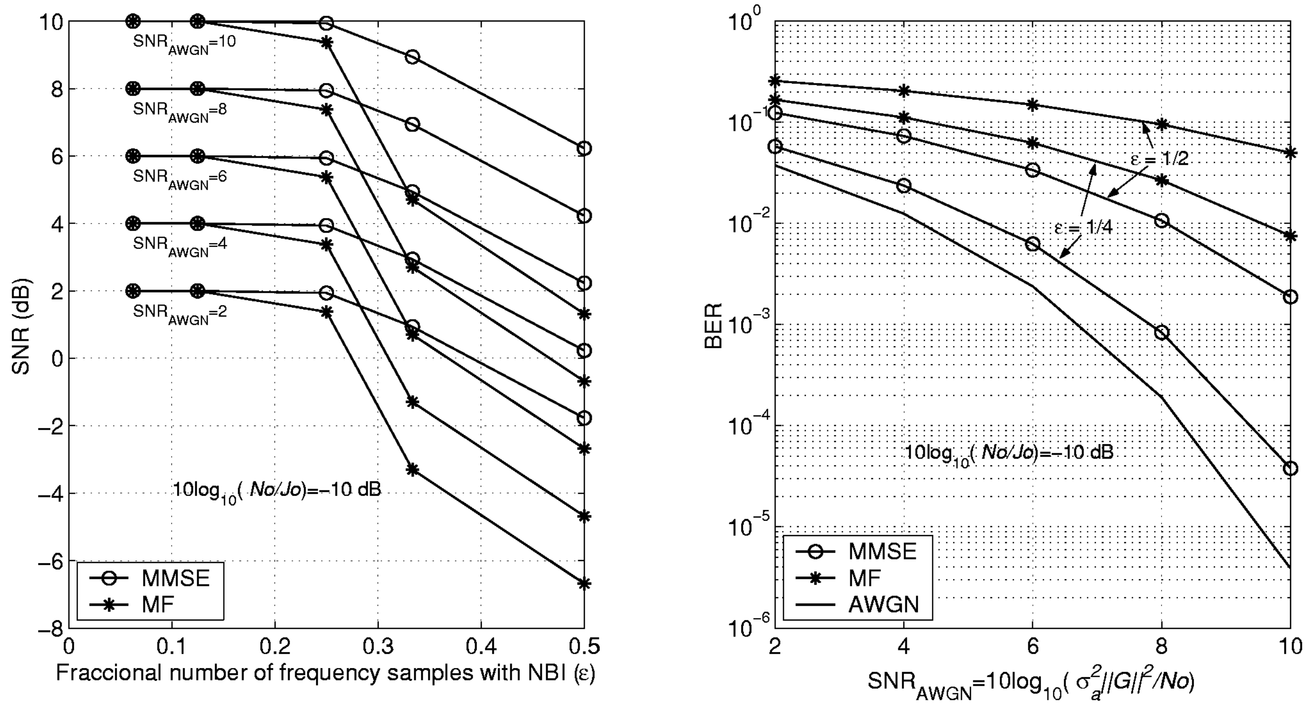

Fig. 4. Comparison of matched filter (MF) and MMSE receivers. (a) SNR vs. ε of MF and MMSE receivers parameterized by $\text{SNR}_{\text{AWGN}} = 10\log_{10}(2\sigma_a^2\|G\|^2/N_o)$. (b) BER vs. $\text{SNR}_{\text{AWGN}} = 10\log_{10}(2\sigma_a^2\|G\|^2/N_o)$ of MF and MMSE receivers for $\varepsilon = 1/4$ and $\varepsilon = 1/2$.

receiver outperforms the MF receiver thanks to the time-frequency resolution provided by the N frequency samples taken every T_c seconds from the received signal and the knowledge of which of those samples were affected by NBI.

5. Conclusions

This paper introduces a multicarrier communication receiver based on analog to digital conversion of the received signal in the frequency domain. The proposed receiver architecture channelizes the spectrum of the received signal by taking N samples of it every $\Delta F_c = 1/T_c$ Hz, where T_c is the A/D conversion-time. The receiver allows for a proper design of the parameters T_c and N, which determines the speed and the system complexity. The favorable trade-off between T_c and N provides a solution to the challenging problems found in the analog to digital conversion needed at the receive end of high-speed communications systems that use signals with very large bandwidths. The proposed receiver possesses advantages of great interest in broadband communication systems including robustness to frequency offset. A narrow band interference rejection method based on the MMSE solution that exploit the time-frequency resolution provided by the frequency domain ADC shows great potential to combat intentional jamming.

References

[1] R. W. Chang, "Orthogonal frequency divison multiplexing," *U.S. Patent 3,488,445, issued Jan. 6 1970.*

[2] B. R. Saltzberg, "Performance of an efficient data transmision system," *IEEE Trans. Commun. Technol.*, pp. 805–813, Dec. 1967.

[3] I. Kalet, "The multitone channel," *IEEE Transactions on Communications*, pp. 119–124, Feb. 1989.

[4] L. J. Cimini, Jr., "Analysis and simulation of a digital mobile channel using orthogonal frequency division multiplexing," *IEEE Transactions on Communications*, pp. 665–675, Jun. 1985.

[5] S. B. Weistein and P. M. Ebert, "Data transmission by frequency-division multiplexing using the discrete Fourier transform," *IEEE Trans. Commun. Technol.*, vol. COM-19, pp. 628–634, Oct. 1971.

[6] B. Hirosaki, "An orthogonally multiplexed QAM system using the discrete Fourier transform," *IEEE Transactions on Communications*, vol. COM-29, pp. 928–989, Jul. 1981.

[7] S. Hoyos, B. M. Sadler, and G. R. Arce, "High-speed A/D conversion for ultra-wideband signals based on signal projection over basis functions.," *Proceedings of ICASSP 2004, International Conference on Acoustics, Speech and Signal Processing, Montreal, Quebec, Canada, 2004.*, 2004.

[8] S. Hoyos, B. M. Sadler, and G. R. Arce, "Analog to digital conversion of ultra-wideband signals in orthogonal spaces.," *Proceedings of UWBST 2003, IEEE Conference on Ultra Wideband Systems and Technologies, Reston, VA, 2003.*, Nov. 2003.